Propagation of anthropogenic noise in the ocean

Jens M. Hovem and Tron Vedul Tronstad

The Norwegian University of Science and Technology (NTNU), and SINTEF ICT

Trondheim Norway

Abstract— Acoustic modeling technique is used to study long range propagation of airgun signals with emphasis on the low frequencies having impact on fish species of commercial interest, the frequency range from 25 Hz to 300 Hz. The acoustic propagation model is based on ray theory and can deal with range-dependent bathymetry and depth-dependent sound speed profiles. The bottom is modeled with a sediment layer over a solid rock and requires input values for geoacoustic parameters of the sediments layer and the rock with compressional speed, shear speed and absorptions coefficients. The source level and directionality is modeled for an airgun array with an arbitrary number of airguns of different sizes. The model calculates the complex spectrum and the full-waveform time response of the sound field to long distances from which a number of useful field descriptors and measures are derived. The sound pressure level at selected frequencies and the sound exposure level are calculated as function of range and compared with the threshold reaction level based on auditory and startle response levels for cod. A critical distance is defined as the range when the sound levels is lower that the reaction level. The environmental impact on the sound propagation is studied and discussed on the basis of a number of scenarios with different bathymetry, bottom properties and seasonal variations of sound speed profiles. Using realistic values for source level and directivity of an airgun array, the critical distances were found to vary from 8 km to more than 50 km, depending on the sound speed profiles and the degree of bottom interaction, but the values of the critical distance are very sensitive to the assumed value of reaction threshold. The model has been tested and verified on data obtained at a real seismic survey conducted in the summer of 2009 at Vesterålen – Lofoten area (Nordland VII). In this experiment signals were recorded at fixed hydrophone positions as the seismic vessel approached from a maximum distance of 30 km toward the receiving positions. The same situation was modeled using available geological and oceanographic information as input to the acoustic model. The agreement between the real and recorded signals and the model results is good. This indicates that acoustic-biological modeling may be useful in the design and planning of seismic surveys to minimize the conflict between surveying and fishing.

Paper presented at the 35th Scandinavian Symposium on Physical Acoustics, 29th January - 1th February 2012, Geilo, Norway.

1 Introduction

Oceans environment are noisy because acoustic waves can propagate to long distances due to the relative low attenuation of sound in water compared, for instance, to sound in air. The natural ambient acoustic noise is mainly generated by wind-driven oceans waves and rain. In addition there are a wide variety of anthropogenic noise sources, shipping noise, noise generated from piling and drilling, noise from subsea oil/gas processing equipment and wind mills. There are also the acoustic signals deliberately sent out for a purpose, such as by active sonar, especially high power military sonar, and air guns used in marine seismic exploration. Anthropogenic noise often dominates over the natural ambient noise, especially in the low frequency band from approximately from 10 Hz and upwards to 1000 Hz, or more, Chapman and Hawkins, (1973), Popper, et al. (2003), Simmonds and MacLennan (2004). This frequency band of emission coincides with the frequencies of perception of sea mammals and fish and may therefore affect their natural activities, or even cause physical damages. An example is seismic exploration for oil and gas in certain areas where there also is important commercial fishing interest. This is the case in the North Sea and the Norwegian Sea with on-going conflicts between seismic exploration and fishing. Studies have demonstrated the sound of air-guns signals may exceed the threshold for alarm responses leading to increased fish activity and to changes in schooling and water position up to a distance of 30-50 km resulting in reduced catches.

This has raised questions and demands for imposing rules and restriction on the seismic surveys such that the impact on fishing is minimized. This could be by requiring a minimum distance to fishing activities, or to restrict the surveys to times of the year with no fishing. The critical issue is to establish the rules and to define the minimum distance. Evidently this must be based on both biological knowledge and knowledge and experience in sound propagation in the oceans.

The biological issue is to understand the features of the sound that triggers reactions or changes in fish behavior. Biological information may be obtained from measurements and observation of a few fishes in controlled condition with fish in captivity in pens or tanks, with the obvious risk of not observing the natural reactions typical for free swimming fish. Auditory threshold values as function for frequency are found in the literature for different species and these values are obtained by exposing fish to harmonic signal. A startle threshold can be defined as the sound level the cause strong and rapid reactions directed away from the sound source. The values that exists the startle threshold levels are about 60-70 dB higher than the auditory levels, Eaton et al. (1995), Karlsen et al. (2007). However, it is important to note that the fish is likely to show other types of behavioral changes at lower sound levels than those causing startle responses, Pearson et al. (1992).

The acoustic issue is to understand the physics of low frequency propagation in the ocean and how the long-range propagation depends on the environments. The propagation of underwater sound depends on the environmental conditions, in particular the oceanographic parameters, the topography of the seafloor and the physical properties of the bottom. For instance, during winter seasons in northern waters there is generally a sound speed minimum near the sea surface resulting in an acoustic surface channel where signals from a shallow source propagate with little attenuation to large distances. In other areas, and at

other seasons, the conditions may be entirely different, perhaps with downward refraction and strong bottom interactions with a significant portion of the energy disappearing into the bottom. Most of the knowledge we have today on these issues is developed by military research and development in connection with passive sonar to detect submarines at large distances, which involves about the same frequency band and distances as relevant to disturbances and effects on fish behavior.

It is important to distinguish between stationary broad band noises from for instance a passing ship and the impulsive noise from an airgun or other similar sources. First it is not clear to translate a fish reaction to a steady harmonic tone or a burst of tone to the reaction of the impulsive sound from a nearby airgun. At longer ranges we are dealing with the propagation an oceanic waveguide with multiple reflections from the sea and bottom causing a significant time spread of the received signal that may last several seconds. In such situations the peak pressure is a time-space varying consequence of the coherent effects of multi-path contributions and bandwidth. Furthermore there are often confusions and misunderstanding with the respect to the characterization of sound and source levels, in particular for transient and impulsive sound. Carey (2006) has written a summary paper on this problem and defined a number of matrices, units and recommended practices.

To assess these factors quantitatively it is necessarily to use mathematical /numerical modeling tools that can take all the effects of the oceanography, the bathymetry and the geophysical properties of the bottom into account. Modeling of propagation conditions has always been an important issue in underwater acoustics and there exists a wide variety of mathematical/numerical models based on different approaches. The most common models are based ray theory, expansion in normal modes, models based on wave number integration technique and models based on the solution of the parabolic equation. For an overview of these models and for further references, see Jensen et al. (1993). Although the effects of anthropogenic noise on marine life is an active field of research and has high public interest, it is surprising that the propagation of sound to large distances are hardly mention in the works dealing with bioacoustics. Noteworthy exceptions are the two companion papers by Erbe and Farmer [2000(a) and 2000(b)] where they first presented a software model to estimate impact zones on marine mammals and then applied the model to case of icebreakers affecting Beluga whales.

This paper describes the use acoustic modeling technique to study long range propagation of impulsive sound with emphasis on the low frequencies having impact on fish species of commercial interest, the frequency range from 25 Hz to 400 Hz. After first describing the model and the required inputs, modeled results are compared with results obtained from a joint seismic-acoustic survey conducted in the summer of 2009 at Vesterålen – Lofoten area (Nordland VII). In this experiment signals were recorded at a fixed hydrophone positions as the seismic vessel approached from a maximum distance of 30 km toward the receiving positions. The same situation was modeled using available geological and oceanographic information as input to the acoustic model. The agreement between the real and recorded signals and the model results is good, Tronstad and Hovem (2011), Hovem and Tronstad (2012).

2 Model description

PlaneRay is a ray tracing propagation model that calculates the sound field by coherent addition of eigenray contribution. The crucial task in this type of ray modelling is to find the all the significant eigenrays connecting a source position with the receiver positions. The approach used in PlaneRay is initially to launch a high number of rays and calculates calculate their trajectories together with the travel times and information on where the rays have been reflected from the surface and bottom or gone through turning points. This information, the ray history, is stored in the computer for use in all the following calculations. Subsequently, and using the stored ray history the trajectories, travel times and amplitudes of the eigenrays, within the span of initial angles rays, are found by a special sorting and interpolation routine.

The contributions of all the eigenrays are coherently summed to produce the frequency-domain transfer function for propagation between the source and receivers. The time response is subsequently calculated by multiplying with the frequency function of the source signal and Fourier transformation. A useful feature of sorting and interpolation scheme is the automatic sorting and separations of the different types of ray history, which enables the user to study the various multipath contributions separately. The PlaneRay model has been extensively tested against the OASES (SAFARI) model by Schmidt (1987 and found to be sufficient accurate for frequencies above 25 Hz, which is sufficient for application to fish of interest to commercial fishing. More information on the PlaneRay Model can be found in reports and articles by Hovem (2008, 2011). In this paper we concentrate on the use of the model for prediction sound fields from at different environmental conditions.

The inputs to the model are:

(1) A sound speed profile i.e. sound speed as function of depth. Only one profile is accepted and therefore range dependency in the sound speed cannot be treated.
(2) A bathymetry chart from which depth versus range can be extracted.
(3) A description of the seafloor, possible layered, with sound speed density and abortions coefficients for each layer.
(4) A record or model of the sound source as function of frequency and radiation direction

Items (1) and (2) are normally easy to obtain, either by in situ measurements or from national or interactional data banks. Seafloor information can be more difficult to obtain except for verbal descriptions such as gravel, sand or silt etc. There exist several papers in the literature that gives relevant acoustic values for different types of bottom materials, Hamilton (1987), Hamilton and Backman (1982).

2.1. Characterization of sound fields and propagation conditions

The program calculates the transmission loss as function of frequency and range to receivers at the same depth. In order to understand and compare the transmission loss for the various conditions it is useful to have a common reference. In free space the geometrical loss is that of spherical spreading with which the

sound intensity decays proportionally to distance squared. In an ideal waveguide with constant water depth and sound speed the geometrical loss follows a cylindrical spreading law with the sound pressure decays proportionally with distance. It follows that the geometrical spreading in an ideal waveguide may be approximated with a spherical spreading law at short distance and cylindrical spreading at longer distance. A combination of the two spreading laws may be expressed by the equation

$$\mathrm{TL} = 10\log_{10}\left[r^2 \left(1 + \frac{r^2}{r_t^2} \right)^{-\frac{1}{2}} \right]. \tag{1}$$

This expression gives the asymptotic behavior

$$\mathrm{TL} = \begin{cases} 20\log_{10}(r), & r \le r_t \\ 20\log_{10}(r_t) + 10\log_{10}\left(\dfrac{r}{r_t} \right), & r > r_t. \end{cases} \tag{2}$$

In these equations r_t is a transition range where the transmission loss goes from spherical close to the source and to cylindrical at long ranges. A reasonable value for r_t is a value close to the water depth. Equation (2) may be used for rough calculation of the transmission loss, but is not included and neither are effects of oceanography and bathymetry. Frequency dependent acoustic absorption in the water is implemented using the expression of Francois and Garrison (1982).

The sound exposure level SEL is an energy (E) measure obtained by integrating the square of the sound pressure $p^2(t)$ and normalize with respect a reference sound pressure and an exposure time t_{ref}

$$\begin{aligned} SEL &= 10\log_{10}\left(\frac{E}{p_{ref}^2 t_{ref}} \right) \\ E &= \int p^2(t)\, dt \end{aligned} \tag{3}$$

The reference sound pressure p_{ref} is chosen to be 1μPa and the reference time t_{ref} equal to one second. The SEL values and the spectral levels of selected frequency components may be used to characterize the loudness of airgun sound and to compare with assumed reaction thresholds of different species of fish. Since the model calculates the complete waveform of the sound other measures can easily be implemented.

2.2. Source pulse and array directivity

Information on the source signal and directivity is required to determine the sound field. Records of source signal may be available for the surveyor, but the program requires far field directional measurements without contamination by reflections from the sea surface or from the bottom. In the absence of such information, the model uses a synthetic source signal in the form of a Ricker pulse frequently used in seismology, Sherif and Geldhart (1959). An example of a Ricker pulse and its frequency spectrum is shown in Figure 1.

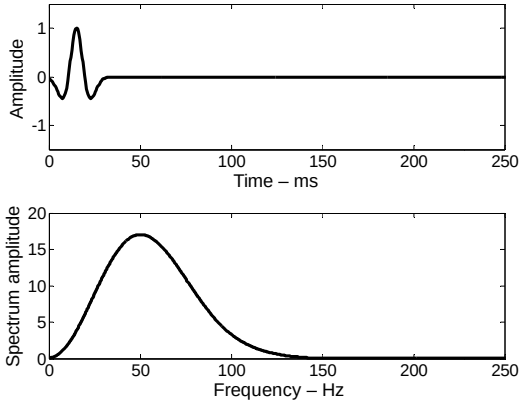

Figure 1. Time pulse and frequency spectrum of the 50 Hz Ricker source signal used in the discussion.

2.3. Airgun array directivity

A typical layout used in commercial seismic surveys is shown in Figure 2 with N_x guns in the towing direction and N_y guns in the cross direction with. Typically, there may be around 30 active guns of different sizes distribute in over an area of 20 x 25 m. Considering the size of the airgun array and the wavelengths it is clear that the directivity of the airgun array is important and must be include in the calculations of the acoustic field.

With reference to Figure 2 the positions of the guns are denoted by (x_n,y_n) and source strengths are $Q_{n,m}(\omega)$. The signal from the array in the farfield as function of elevation angle θ, the azimuth angel φ, and the (angular) frequency ω, can be expressed by

$$S(\omega,\theta,\varphi) = \sum_{n,m} Q_{n,m}(\omega) \exp\left[-\frac{\omega}{c} i \left(x_{n,m} \cos\theta \cos\varphi + y_{n,m} \cos\theta \sin\varphi \right) \right]. \quad (4)$$

In the in-line direction where the azimuth angel φ is zero, this reduces to a line array of sources

$$S(\omega,\theta,\varphi=0)=\sum_{n,m}Q_{n,m}(\omega)\exp\left[-\frac{\omega}{c}i(x_n\cos\theta)\right]. \tag{5}$$

In the across direction perpendicular to the towing direction $\varphi = \pi/2$ with

$$S(\omega,\theta,\varphi=\pi/2)=\sum_{n,m}Q_{n,m}(\omega)\exp\left[-\frac{\omega}{c}i(y_m\cos\theta)\right], \tag{6}$$

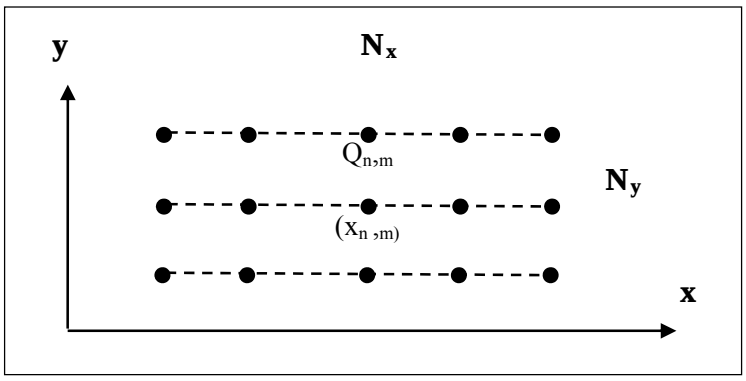

Figure 2. Air gun array with N_y lines each with N_x guns

Equations (4) and (5) are general expressions valid for any number of sources with different frequency spectrum and locations, but requires that the source functions are known for each of the guns in the arrays. In cases that such detailed information is not available the following approach is used to estimate the directivity function of the airgun array. The approach is based on the assumption that all the guns in the array produces pulses of the same shape, but with a peak pressure amplitude that depends only on volume of the pressure chamber, given that the pressure in the all guns are the same. Thereby the source strengths in the above equations for the beam pattern are replaced by volume weights

$$Q_{n,m}(\omega)=Q_0(\omega)V_{n,m}^{\gamma}\ . \tag{7}$$

In this expression $V_{n,m}$ is the normalized volume of the individual guns and the exponent γ has the value of 1/3 [Caldwell and Dragoset (2000)]. $Q_0(\omega)$ is a frequency function of the common source signal, which here is taken as a Ricker pulse as described in the previous paragraph. This approach is a relatively poor approximation to the signature from a single air gun, but a reasonable approximation to the signature of all the guns combined since the firing times and the sizes of the individual guns are selected and synchronized to produce a single sharp pules without with a minimum of bubble oscillations.

In the in-line direction the transmitted signal from the array is

$$S(\omega,\theta,\varphi=0)=Q_0(\omega)\sum_{n=1}^{N_x} q_n \exp\left[-\frac{\omega}{c} i\left(x_n \cos\theta\right)\right]. \tag{8}$$

Where q_n represent the relative strengths of the individual airgun sources and x_n are their positions along the x-axis. The far field directivity function as function of elevation angle and frequency is then

$$B(\omega,\theta)=\sum_{n=1}^{N_x} q_n \exp\left[-\frac{\omega}{c} i\left(x_n \cos\theta\right)\right]. \tag{9}$$

As an example we the values from an airgun array used in 2009 in a seismic survey at Nordland VII field are

$$\begin{aligned} q_n &= [0.2308\ 0.1963\ \ 0.1679\ \ 0.1656\ 0.1350\ 0.1044], \\ x_n &= [0\ \ 5.0\ \ 7.5\ \ 11.0\ \ 13.0\ \ 16.0] \end{aligned} \tag{10}$$

Figure 3 shows the resulting beam pattern for the frequencies of 50 Hz and 100 Hz. For 50 Hz the reduction in transmitted level in the horizontal directions is about -5 dB compared to level in the vertical direction, At 100 Hz there is a side lobe reaching a level of about – 15 dB compared with the level in vertical direction. The maximum amplitude is in the vertical direction and in the modeling of the time and frequency responses the maximum peak amplitude is scaled up to the level specified by the surveyor, which is 255 dB re 1 μPa in the case of the Nordland VII survey. From Figure 3 is evident that the array directivity is important for the accurate calculations of the sound field.

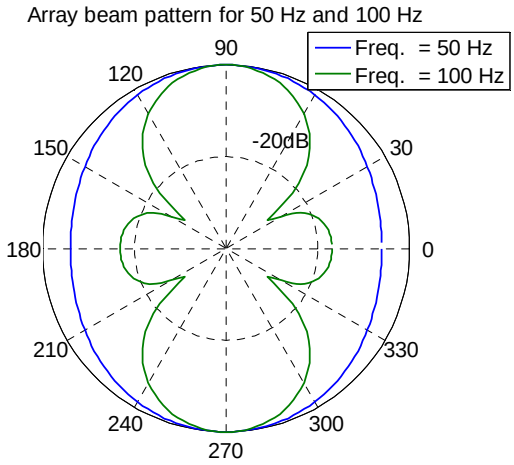

Figure 3. Modeled directivity of the airgun array for 50 Hz and 100 Hz calculated for the weights and positions given by equation (10)

2.4. The bio-acoustic model

The minimum distance between the source and a fish population required to avoid any significant reaction or change in behavior is defined as the critical distance. The actual reaction threshold for the various species is difficult to ascertain and is an area of active research not discussed here [Simmonds, J and D. MacLennan (2004)]. However, the problem with defining a reaction threshold can be illuminated with Figure 4 showing the auditory and startle threshold for Atlantic cod. At 50 Hz the auditory threshold is about $5 \cdot 10^3$ μPa and the startle response threshold is about $5 \cdot 10^7$ μPa. Note that the startle sound pressure threshold level in Figure 4 is about 60-70 dB higher than the auditory level. Startle responses are strong and rapid reactions directed away from the sound source, but the fish is likely to show other types of behavioral changes at lower sound levels than those causing startle response. Some studies have shown behavioral changes and alarm responses at sound levels 20-25 dB lower than the threshold for startle responses. To give an indication of possible maximum interaction ranges, we have in this study assumed a reaction threshold of $3 \cdot 10^7$ μPa which translates into 150 dB re $1 \mu Pa$., which is close to startle threshold. We have also neglected the frequency dependence in the reaction threshold since the dependence is weak in the frequency band of primary interest. This threshold value is only intended for discussion and must not in any case be considered as more than an illustration.

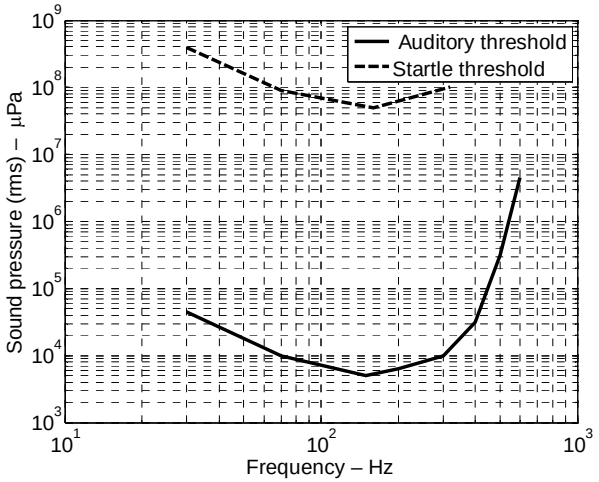

Figure 4. Auditory and startle threshold for Atlantic cod. Auditory threshold data are from Chapman and Hawkins (1973) and Chapman (1973). Startle threshold data are from Karlsen et al. (2007).

3 Experimental verification Nordland VII

The Norwegian Petroleum Directorate (NPD) conducted a seismic survey off the coasts of Vesterålen in the summer of 2009. This was a regular commercial marine seismic survey, but in addition other observations and measurements were conducted to obtain calibrated records of the airgun sounds and to observe the degree to which commercial fishes was affected, Løkkeborg et al., (2010). The chosen line for the analysis, line 1344, is about 30 km long and passing directly above a hydrophone at a depth of 83 m recording the sound received from the approaching seismic vessel towing an airgun array at 6 m depth.

The input for the modeling is the average sound speed profiles measured at the day of the experiment and the bathymetry extracted for official sea maps. Figure 5 shows the sound speed profile and the bathymetry along the seismic line and the ray traces from a source at 6 m depth out to distance of more than 30 km.

Accurate information about the acoustic properties of the sea floor can be more difficult to obtained, as indicated before. In this case we used information from the Geological Survey of Norway (NGO), (2010) where the bottom in the area is characterized as gravel. The tabulated values of Hamilton [1987] suggested the following values to use in the modeling of line 1344. Compressional wave speed 2000 m/s, bottom density 2500 kg/m^3, compressional wave attenuation: 0.1 dB/λ, shear wave speed: 600 m/s, shear wave attenuation 1.0 dB/λ.

Figure 6 shows the measured and modeled sound exposure level (SEL) as function of range using the values quoted above with no further attempts to obtain a better fit with the measured values. The agreement between the measured and modeled levels is good, both showing that level deceases sharply with the increasing depth at ranges over about 7 km. The measured and modeled SEL values are compared with the assumed reaction threshold given in equation (3), indication a critical distance of 5-6 km. Observing the fish behavior and fishing indicate that there were no or little reactions at longer distances than this

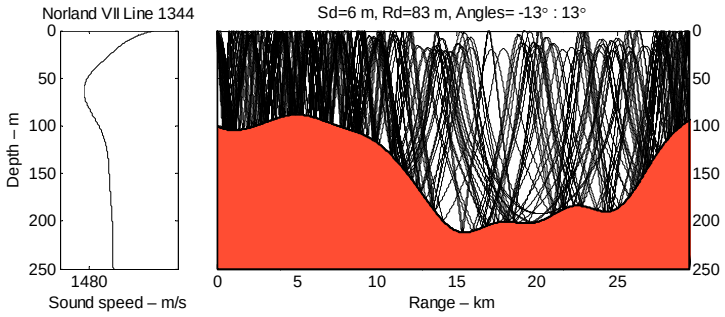

Figure 5. Modeled sound field from a source at 6 m depth to a distance up to 30 km.

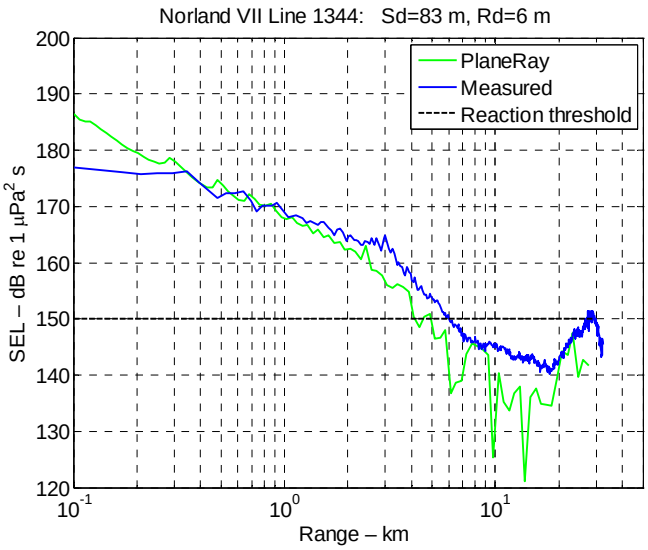

Figure 6. Measured and modeled sound exposure level (SEL) as function of range for line 1344 in Nordland VII with comparison with the assumed SEL threshold level of 150 dB re $1\mu Pa^2 s$.

The sharp decrease in level is partly caused by the increasing water depth, but also losses associated with the bottom reflections. The values for the sound speed and attenuation yield the bottom reflection loss shown in Figure 7. The sound speed of 2500 m/s gives a critical angle of 42°, but as can be seen from the figure there is a significant bottom reflection loss at lower angles. This propagation loss is caused by loss of energy due to sound absorption and conversion to shear waves in the bottom. Most important is the relatively high value of the shear speed and attenuation (600 m/s) and dB/λ).

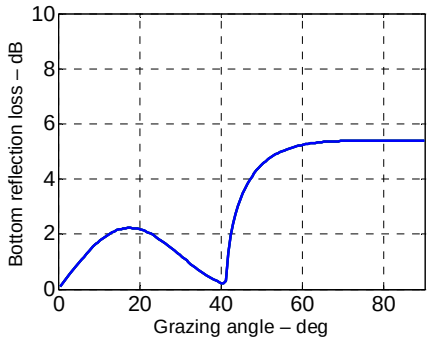

Figure 7. Bottom reflection loss for values used to model line 1344. Compressional wave speed: 2000 m/s, bottom density 2500 kg/m^3, compressional wave attenuation 0.1 dB/λ, shear wave speed 600 m/s and shear wave attenuation 1.0 dB/λ

This is further illustrated by Figure 8 showing the transmission loss as function of range and for the cases when the shear speed in the bottom is as 600 m/s compared with the loss of zero shear speed in the bottom. The differences between the curves displayed in the two figures is the shear wave conversion loss and at ranges longer than 10 km the loss is about 20 dB. The dotted line is the geometrical transmission loss of equation (1), which gives a slope of 10 log(r) for ranges longer than the water depth at the source.

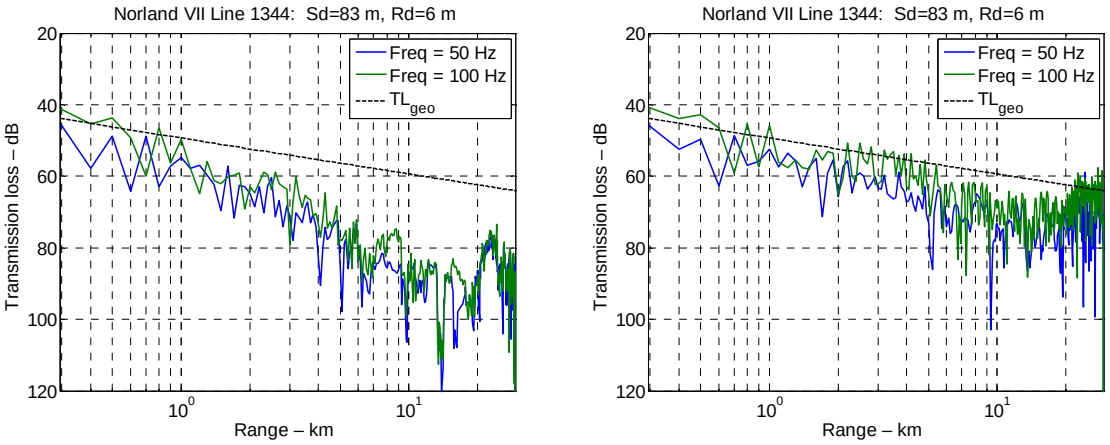

Figure 8. Modeled transmission loss for Nordland VII as function of range and for the frequencies of 50 Hz and 100 Hz: Left with for 600 m/s shear speed, and right with zero shear speed.

4 The environment

The purpose of this work is to develop a model for prediction the sound field from an impulsive source to distances relevant for eliciting fish interaction and disturbances for fishing activities. To demonstrate the use of the model and to illustrate how the environmental factors of the oceanography, the bathometry and structure and composition of bottom we constructed a set of hypothetic, but realistic, scenarios with different sound speed profiles, bathymetry and bottom properties. In all the scenarios the source depth is fixed to 6 meter as typical for a seismic airgun, but both deep and shallow receiving depths are considered.

4.1 The sound speed profiles

The sound speed profiles used in the simulations were measured at Halten in the Norwegian Sea (64°N, 10° E) at different seasons at different years. The selected profiles are shown in Figure 9. In the following we present only the results from the February and the July profiles since these two profiles are typical for the extreme variation that can be expected. The ray traces for the two selected sound profiles for winter (February) and summer (July) conditions are Figure 14.

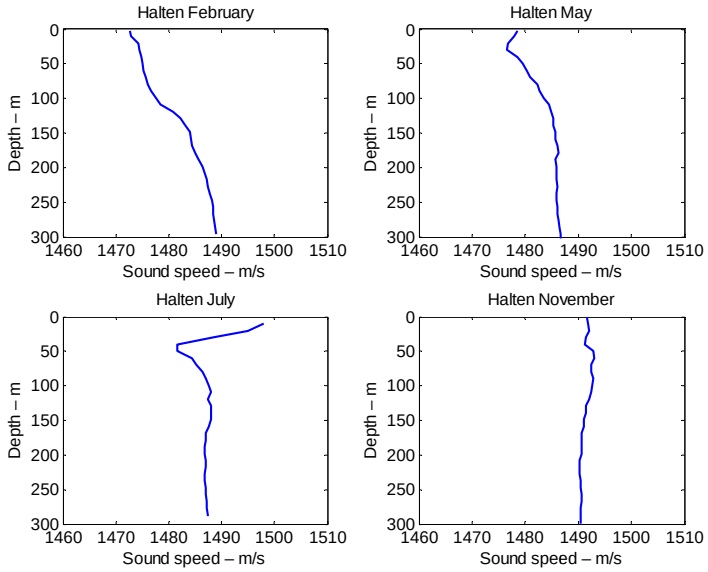

Figure 9. Measured sound speed profiles at in the Norwegian Sea (Halten) for the months of February, May, July and November

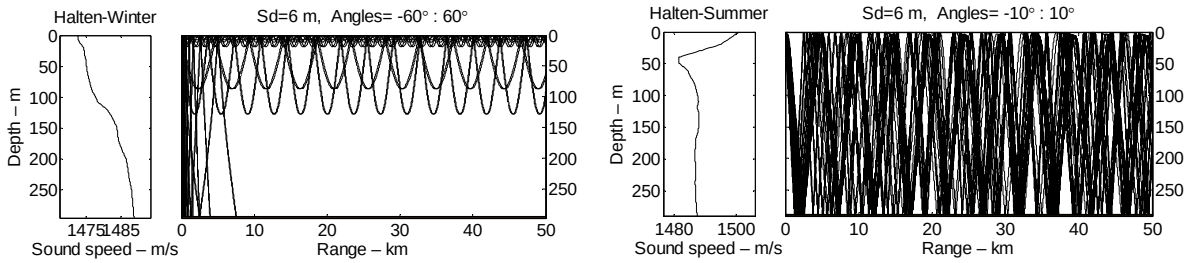

Figure 10. Ray traces from a source at 6 m depth for winter and summer conditions at Halten in the Norwegian Sea, Only a few rays are shown to give a simple impression of the impact of the sound profiles variation,

The February profile is a typical winter profile where colder water nearest the surface gives a positive sound speed gradient, increasing sound speed with depth, over the whole water column. The consequence is upward refraction with concentration of sound in the upper part of water column. The bottom interaction is weak since the rays are bent upwards and the propagation is only weakly dependent on the acoustic properties of the bottom

The July profile is governed by a relative high surface temperature decreasing with depth and resulting in a sound speed minimum at a certain depth, in this case at about 50 m. A sound speed minimum creates a sound channel where the sound is trapped and propagates to very long distances. Except for propagation in the sound cannel most of the sound is reflected many times from the bottom giving a high degree of sensitivity to bottom parameters.

4.2 The bottom model

As already demonstrated the bottom reflection losses are important for low frequency sound propagation and in many cases is the determining factor for how far the noise may affect the behavior of fish. The bottom model used in this study has a sediment layer over a solid rock half space as shown in Figure 11. The sediment layer with thickness D is modeled as fluid with sound speed c_s and density ρ_s. The rock has sound speed c_{rp}, shear speed c_{rs} and density ρ_r. All waves are attenuated with absorption coefficients α_s, α_{rp} and α_{rs}, measured in dB wavelength, respectively for three wave types.

Figure 12 shows a contour plot of the bottom reflection loss (dB) as function of incident grazing angle and frequency. The parameters are, c_s= 1700 m/s, c_{rp}= 3000 m/s, c_{rs}= 600 m/s, ρ_s = 1800 kg/m^3 ρ_r = 2500 kg/m^3, $\alpha_s = \alpha_{rp} = \alpha_{rs} = 0.5/\lambda$. The reflection coefficient and the reflection loss are functions of the product of the acoustic frequency f and layer thickness D represented as the vertical axis in the figure. The reflection loss Figure 12 can therefore be scaled to any layer thickness and frequency.

The reflection loss changes with frequency and for very low frequencies approaches the reflection loss of a homogenous rock bottom, but approaches the reflection loss of a uniform sedimentary bottom at high

frequencies. The two critical angles for the sound speeds of c_s =1700 m/s and c_{rs} = 3000 m/s for the sediment and the rock, respectively 28° and 60° are clearly recognizably in the graph.

With zero shear speed in the rock and zero wave absorptions in the sediment and the rock, the reflection loss is zero for angles smaller than the critical angles, which in this example is 28° and 60° for high and low frequencies, respectively. However, the reflection loss of Figure 11 shows significant losses also in areas of low frequencies and low angles. The losses in these areas are consequences of energy lost by wave absorption and conversion to shear waves in the bottom. Figure 12 (left) shows the low-frequency and low angle area extends up to frequency- layer thickness product of 500 m/s. For a frequency of 50 Hz the propagation is significantly affected by properties down to about 10 m into the bottom.

Propagation of sound at low frequencies are very dependent on bottom reflection losses and this issue has been treated extensively in the literature, as for instance Hovem, Richardson and Stoll (1991.

This study compares the propagation using two bottom types

- Bottom type (I) Homogenous sediment with sound speed 1700 m/s, density 1800kg/m^3 and attenuation 0.5 dB/ wavelength.
- Bottom type (II) Sediment layer with thickness 2 m over solid rock with compressional speed 3000 m/s, shear speed 600 m/s, density 2500 kg/m^3. Both wave types with attenuations equal to 0.5 dB/wavelength.

Bottom type (I) results by setting the thickness of the sediment D to infinity and type (II) is with D=2 m.

Figure 11. Sea bottom model with a sediment layer over a solid rock half space

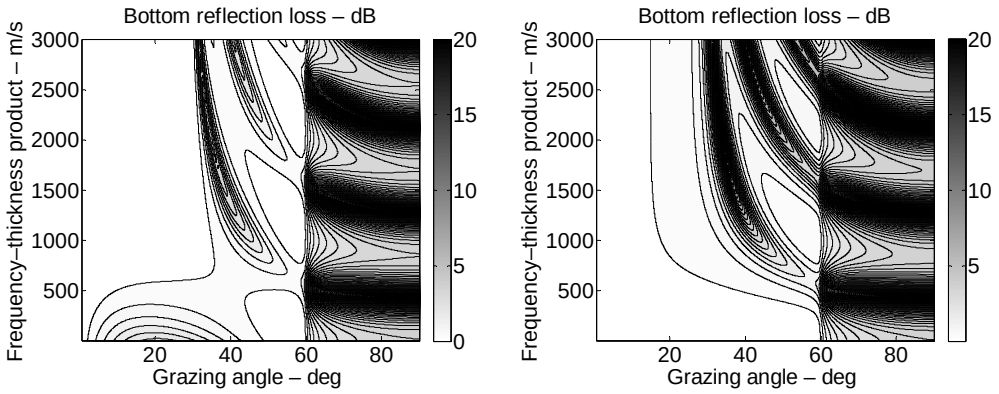

Figure 12. Bottom reflection loss (dB) as function of frequency and incident grazing angle for a layered bottom with a sediment layer over hard rock. The parameters are given in the text.

Figure 12 shows the bottom reflection loss for bottom type(I) and (II) as function of incident grazing angle and for the frequencies of 50 Hz and 100 Hz. For bottom type (I) the reflection loss is independent of frequency and the critical angle is 28° In the following discussion, bottom type (I) is referred to as a low loss bottom and bottom type (II) as a high loss bottom.

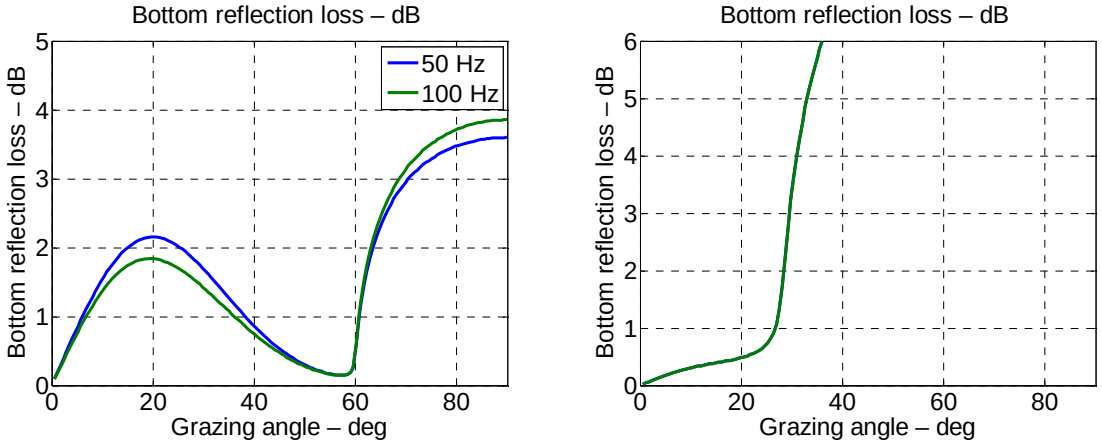

Figure 13. Expanded view of the bottom reflection loss (dB) as function of frequency and the incident grazing angle. Left: Bottom type (II), Right: Bottom type (I), which is independent of frequency. The parameters are given in the text.

4.3 The bathymetry

The effects of the bathymetry are investigated for the downslope and upslope propagation cases depicted in Figure 14. The water depth changes with 150 m over a distance of 30 km having a slope of about 0.5 %. As will be demonstrated, even a gentle slope of the magnitude may significantly influence the propagation and the critical distance

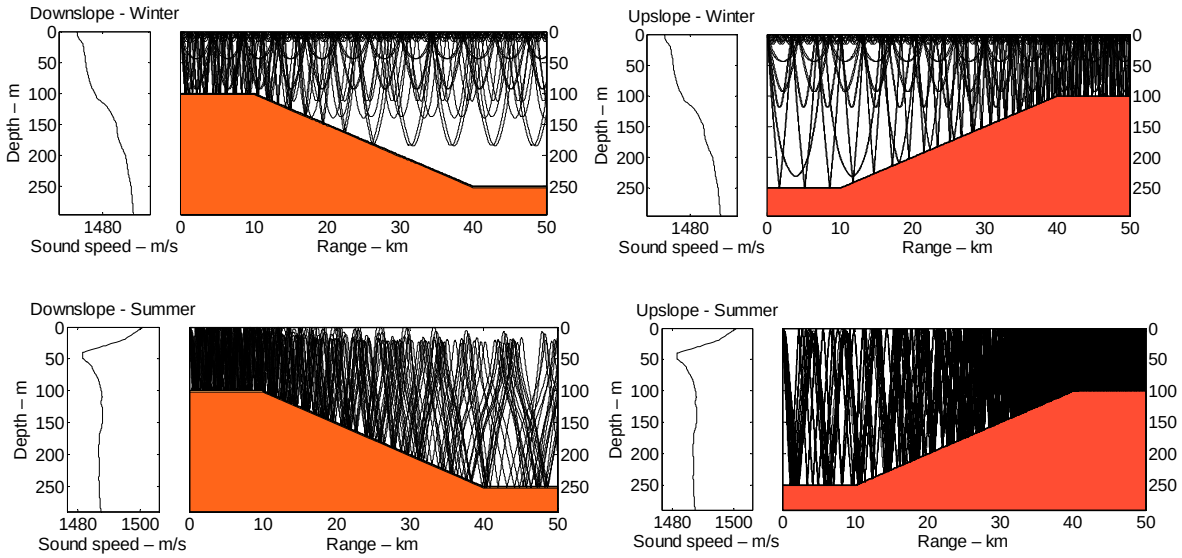

Figure 14. Examples of scenarios for discussing bathymetric effects on long range propagation.

The ray diagrams in Figure 14 shows several interesting and important features. Downslope propagation leads to a thinning of rays causing faster decay of the sound level with range than propagation in waters with constant depth. Upslope propagation yields a concentration of rays with range such that the geometrical propagation loss is initially reduces and the sound level increases with range until a point may be reached where the grazing angles of the rays reach 90°, which signifies a cutoff in propagation. (Back-reflected rays are ignored in the propagation model). In addition there is effect of bottom reflection losses, most pronounced for the winter conditions as observed earlier.

5 Simulation results

This section presents the modeling results for the environments described in section 4. The intention is to demonstrate the importance the three factors of sound speed profile, the bottom composition and bathymetry may impact low frequency propagation both separately and in combination.

5.1 The reference case, the Pekeris waveguide

The first case is the simple case with constant sound speed and constant water depth and with a sediment type bottom modeled as a homogenous fluid, characterized with sound speed, density and attenuation. This case is often referred to as the Pekeris waveguide and may serve as a reference case.

Figure 15 shows the time responses as function of reduced time and range for the two bottom types (I) and (II). The time scale is in reduced time with the gross time delay of the transmission between the source and receiver has been subtracted. The reduced time is defined as

$$t_{red} = t_{real} - \frac{r}{c_{red}}, \tag{11}$$

where t_{real} and t_{red} are the real and reduced times, respectively, r is range and c_{red} is the reduction speed. The actual value of c_{red} is not important as long as the chosen value results in a good display of the time responses.

The red dotted lines in Figure 15 represent an estimate of the duration of the cannel impulse response. This time duration is mainly given by the critical angle of the bottom reflection coefficient. Rays that propagate at angles closer to the horizontal plane than the critical angle experience almost no bottom reflection loss and may therefore propagate to long distances. Rays with steeper angles will experience higher reflection losses and die out more rapidly with range. Thus the time duration of the impulse may be estimated directly by the ratio of sound speeds in the water and the bottom as

$$t_{red} = \frac{r}{c_0}\left(\frac{1}{\cos\theta_{crit}} - 1\right) = r\left(\frac{c_b - c_0}{c_0^2}\right). \tag{12}$$

This estimate of the time duration of the channel impulse response assumes that the bottom is fluid-like, homogenous and flat, but the estimate may also be useful in other cases with moderately range dependent depth and with solid or layered bottom. In the figure the estimated time duration of the impulse response calculated on the basis of the highest wave speed in the bottoms of (I) 1700 m/s and 3000 m/s (II). As can be observed, the time duration or responses may be very long for a hard bottom.

Figure 16 shows the transmission loss as function of range for the two bottom types (I) and (II). Directionality is not included in the plot since this is considered a property of the source and not of the medium. The dotted line is the geometrical transmission loss of equation (1), which gives a slope of 10

log(r) for ranges longer than the water depth at the source. The transmission loss for bottom type (II) with shear wave conversion is significantly higher than for bottom type (I), the difference approaching 10 to 15 dB at the longer ranges. This is as expected from plots of bottom reflection loss in Figure 13

The critical range where the sound level drops below the threshold value of fish reaction can be defined in various ways. We have chosen to use either the SEL values or the levels of selected spectral 50 and 100 Hz. Figure 17 shows the SEL values as function of range calculated for the bottom types (I) and (II) and compared with the assumed threshold value of fish reation. In Figure 18 the spectra lines of 50 Hz and 100 Hz are compared with the same threshold. The difference between the sound level at 50 Hz and 100 Hz is mainly caused by the directivity and the higher source level at 50 Hz than for 100 Hz. The critical range is defined by the crossing with the assumed reaction threshold indicated by the dashed line. For propagation over the low loss bottom (I) the critical range is about 40 km for both criteria whereas the critical range is about 15 km for the bottom type (II).

The SEL value variation with range is important to sensitivity of the critical distance. In this case the low loss bottom type (I) give a slope with range of 10 log (r), the high loss bottom type (II) varies 20 log (r) at the crossings with the reaction threshold.

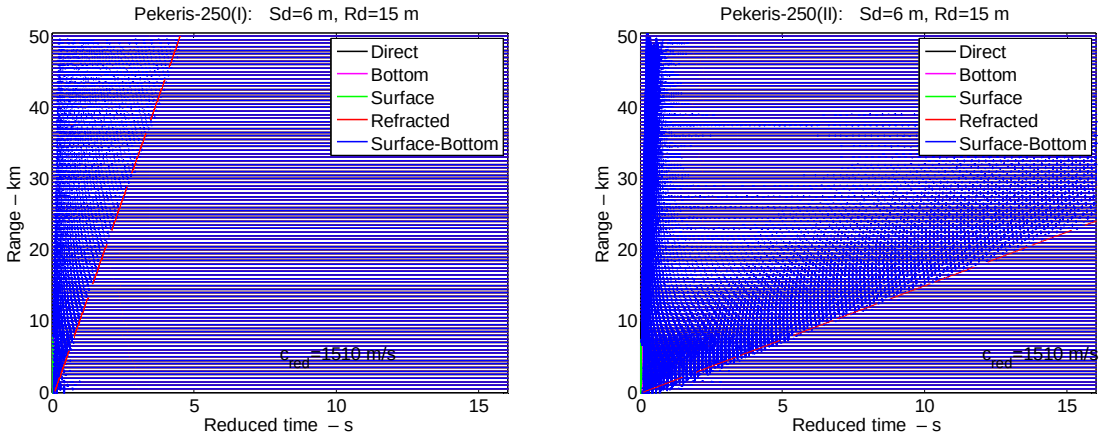

Figure 15. Time responses in a Pekeris waveguide as function of reduced time and range from source receiver calculated for the two bottom types (I) and (II).

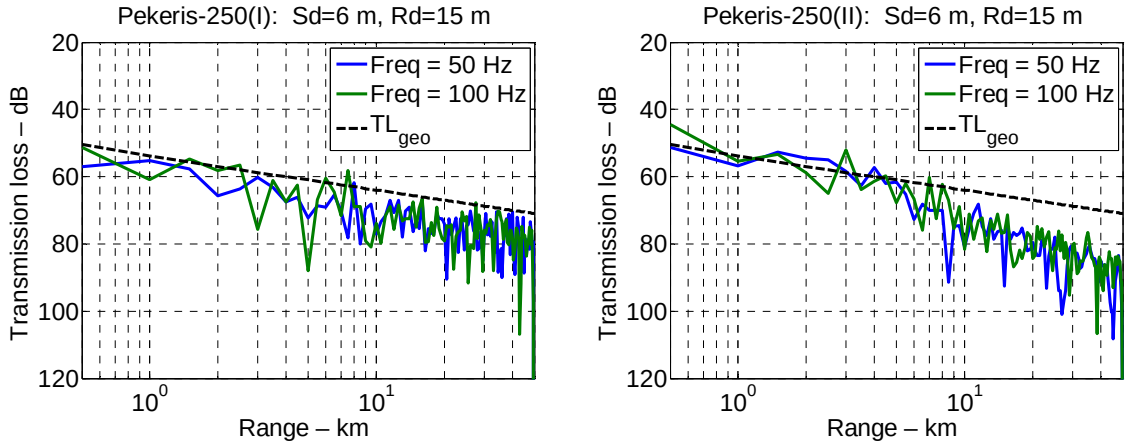

Figure 16. Transmission loss as function of range for the two bottom types (I) and (II). The dotted line is the geometrical transmission loss of equation (1)

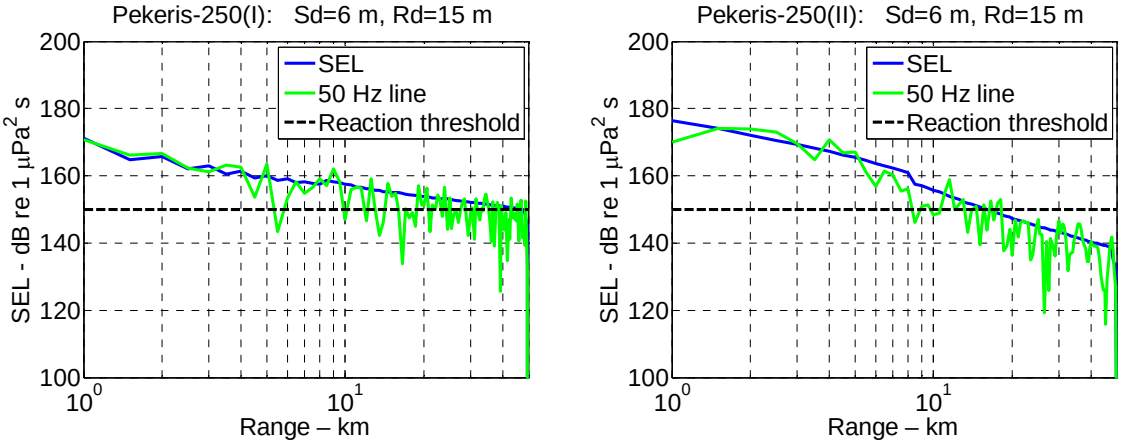

Figure 17. SEL values and spectral valus for 50 Hz as function of range for the Pekeris waveguide calculated for the bottom types (I) and (II). The dashed line is the assumed threshold value of fish reation.

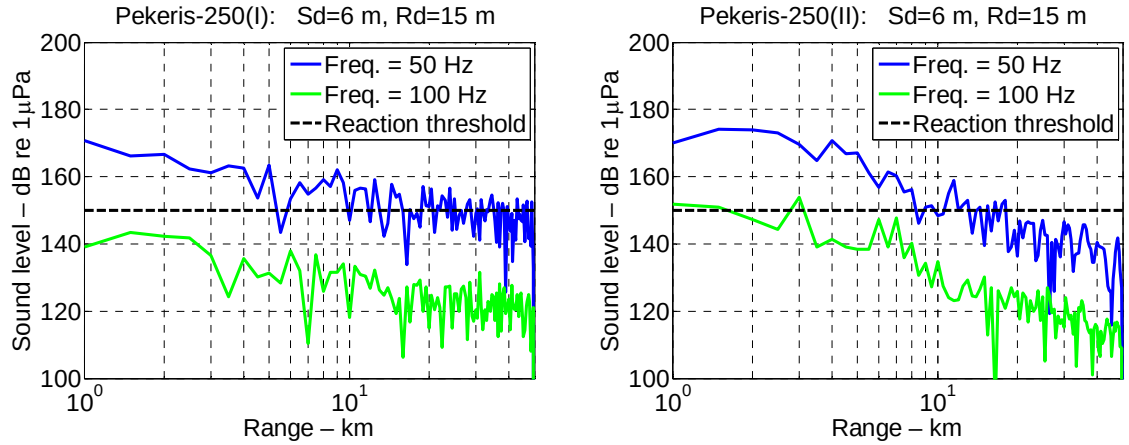

Figure 18. Spectral line values at 50 Hz and 100 Hz as function of range for bottom types (I) and (II). The dashed line is the assumed threshold value of fish reation.

5.2 Propagation under different seasonal condition

The effects of seasonal variations of the environment are illustrated by simulation of propagation at typical summer and winter conditions in the Halten area in Norwegian Sea using the speed profiles of July and February shown in 0Figure 9. This case may serve as example of the propagation effects caused by the combination of sound speed profiles and bottom properties over a flat bottom.

Figure 19 shows the time responses for winter and summer conditions and for the two bottom types (I) and (II). In the winters, the signals from a shallow source propagates mainly in the surface channel being repeatedly reflected from the sea surface and refracted at different depths without striking the bottom. Consequently the bottom composition is not an important factor for the propagation. Under summer conditions the most propagation paths are with bottom reflections and therefore the transmission is strongly dependent on the bottom properties. The influences of the bottom types are also clearly visible in the same way as can see in Figure 15.

Figure 20 shows the SEL values and spectral values at 50 Hz for propagation under summer and winter conditions and for bottom types (I) and (II). Winter conditions give strong transmission to receivers at shallows depth with critical range in excess of 50 km, almost independent of the bottom proerties. For the summer conditions the critical distance is about 20 km for both bottom types (I) and (II).

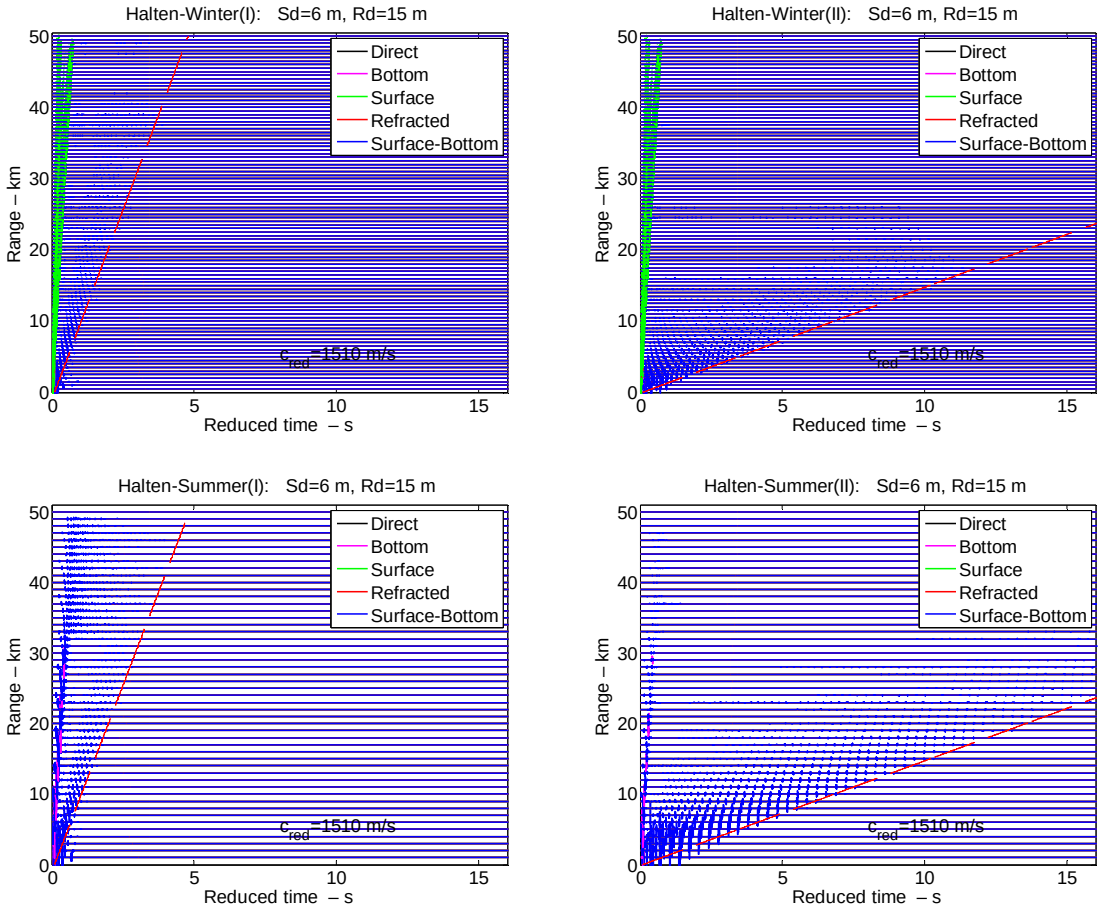

Figure 19. Time responses at Halten as function of reduced time and range for summer and winter conditions calculated for the two bottom types (I) and (II).

Figure 20 shows the SEL values and spectral values at 50 Hz for propagation under summer and winter conditions and for bottom types (I) and (II). Winter conditions give strong transmission to receivers at shallows depth with critical range in excess of 50 km, almost independent of the bottom proerties. For the summer conditions the critical distance is about 20 km for both bottom types (I) and (II).

Figure 21 show the transmission loss as function of range for the frequencies of 50 Hz and 100 Hz. In these plots the directionality and the level of the source are not included. The model results of the propagation loss are significantly different from that of the simple equation (1).

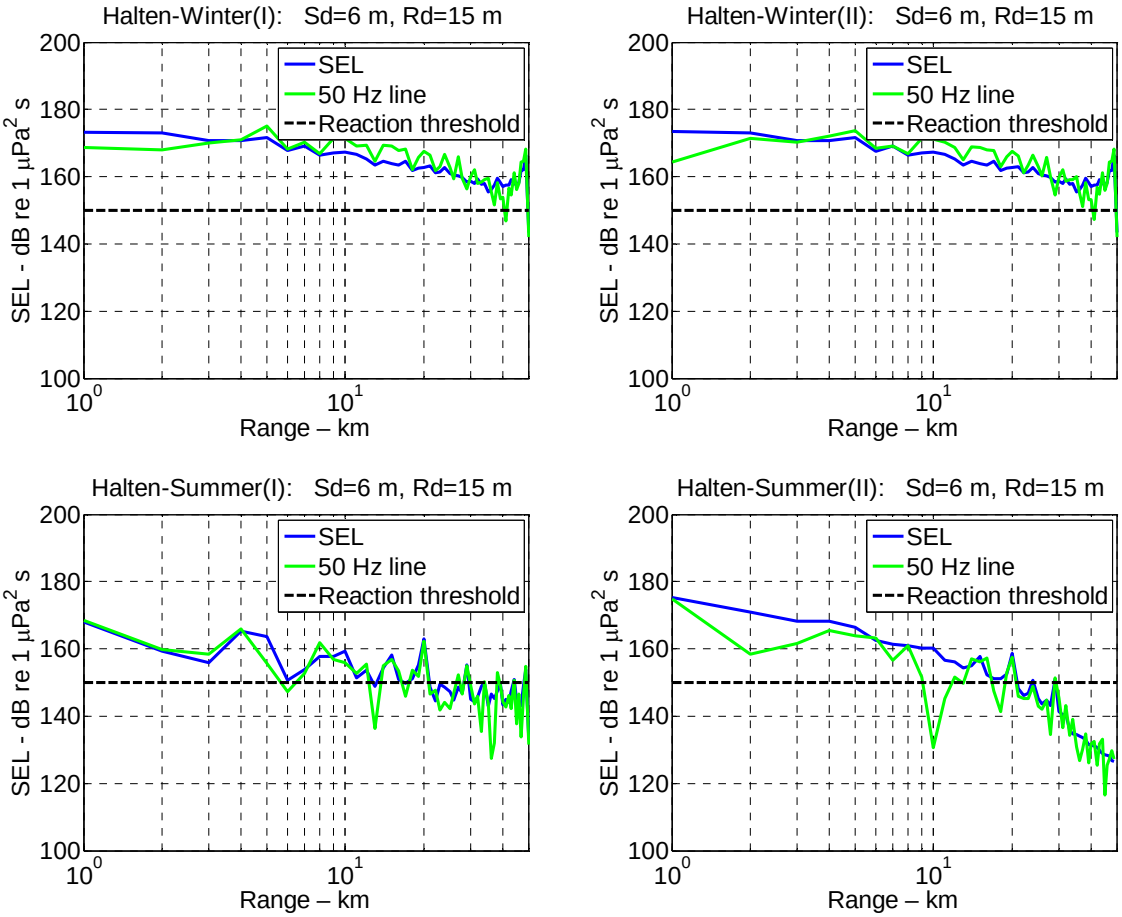

Figure 20. SEL values and spectral values for 50 Hz as function of range for summmer and winter conditions at Halten calculated for the bottom types (I) and (II). The dashed line is the assumed threshold value of fish reaction.

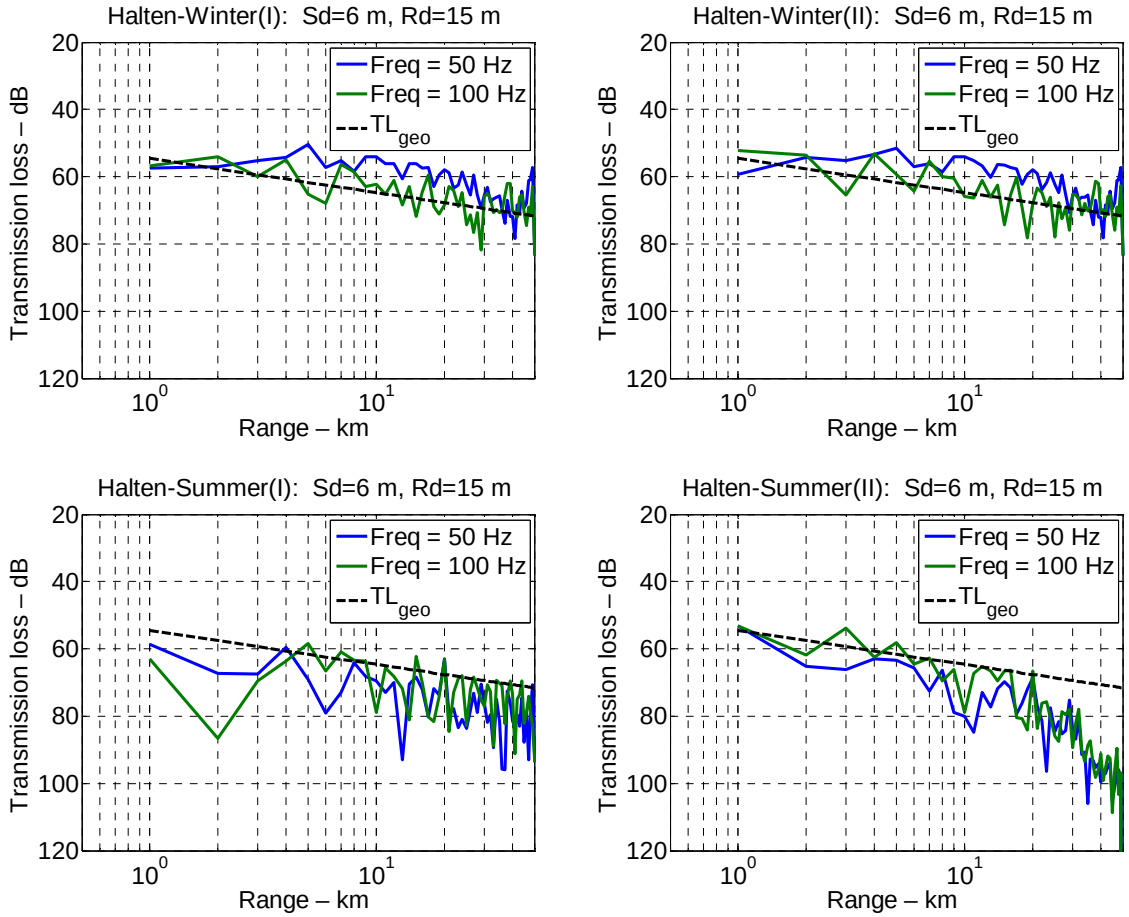

Figure 21. Transmission loss as function of range for winter and summer at Halten for the two bottom types (I) and (II).The dotted line is the geometrical transmission loss of equation (1)

In the cases considered so far the receiver depths are 15 m and the treatment relevant for fish near the sea surface. However in many cases the depth is important for the sound level and this demonstrated by considering receiver at 225 m depth, which is 15 m above the bottom. Figure 22 and Figure 23 show the result for winter condition in the Norwegian Sea, this figures should be compared with Figure 20 showing the winter results for receivers at 15 m depth. The difference is significant and about 10 to 15 dB lower at 225 m depth compared with the levels at 15 m depth. The bottom properties are not very important for the winter conditions as earlier concluded.

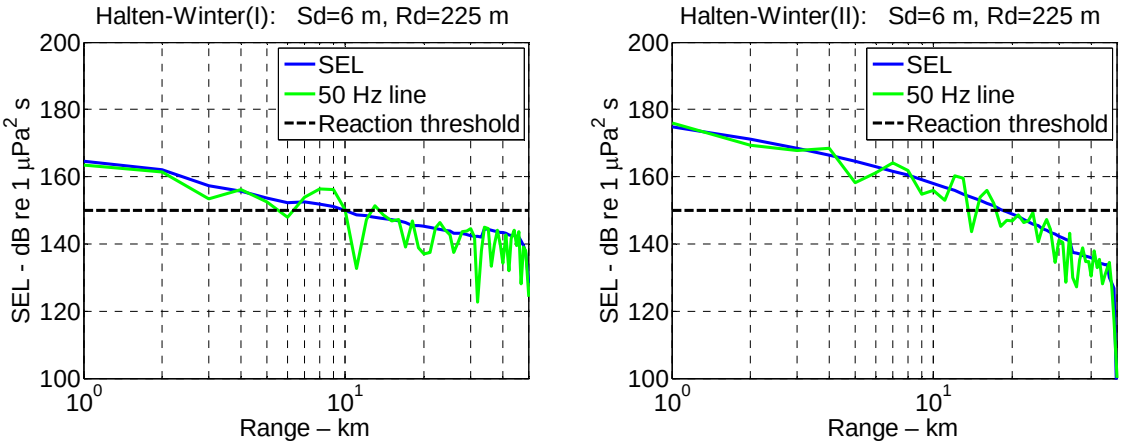

Figure 22. SEL values and spectral values for 50 Hz at 225 m depth as function of range for summmer and winter conditions at Halten calculated for the bottom types (I) and (II). The dashed line is the assumed threshold value of fish reaction.

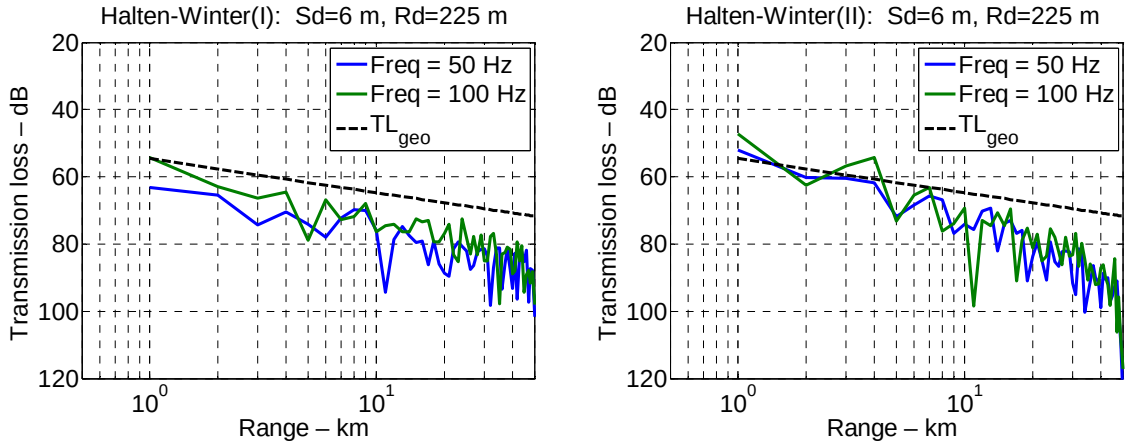

Figure 23. Transmission loss for winter condition in the Norwegian Sea at for the frequencies of 50 Hz and 100 Hz. as function of range a depth of 225 m for bottom types (I) and (II). Directionality is not included. Receiver depth is 225 m

5.3 Bathymetric effects

This section discusses the propagation over down and up sloping bottoms evaluated for winter and summer conditions and for the two bottom types (I) and (II) the scenarios are shown in Figure 14.

Figure 24 shows the results for downslope propagation under summer and winter conditions, respectively, with SEL values and spectral values at 50 Hz as function of range for bottom types (I) and (II). The level of the assumed reaction threshold, indicated by the dashed line, gives a critical distance of about 15 km with bottom type (I) and 8 km with bottom type (II) for both summer and winter conditions.

Figure 25 shows the results for upslope propagation under summer and winter conditions with SEL values and spectral values at 50 Hz as function of range for bottom types (I) and (II). With winter conditions the effect of increasing density of rays is clearly visible with nearly constant levels until 30 km where the cut-off effect takes place independent of the bottom properties. For summer conditions the results are similar, but in this case the bottom properties are more important because of more bottom interaction in the summer than in the winter.

Figure 26 shows the transmission loss as function of range for the frequencies of 50 Hz and 100 Hz for downslope propagation and Figure 27 shows the same for the upslope propagation. In these plots the directionality and the level of the source are not included.

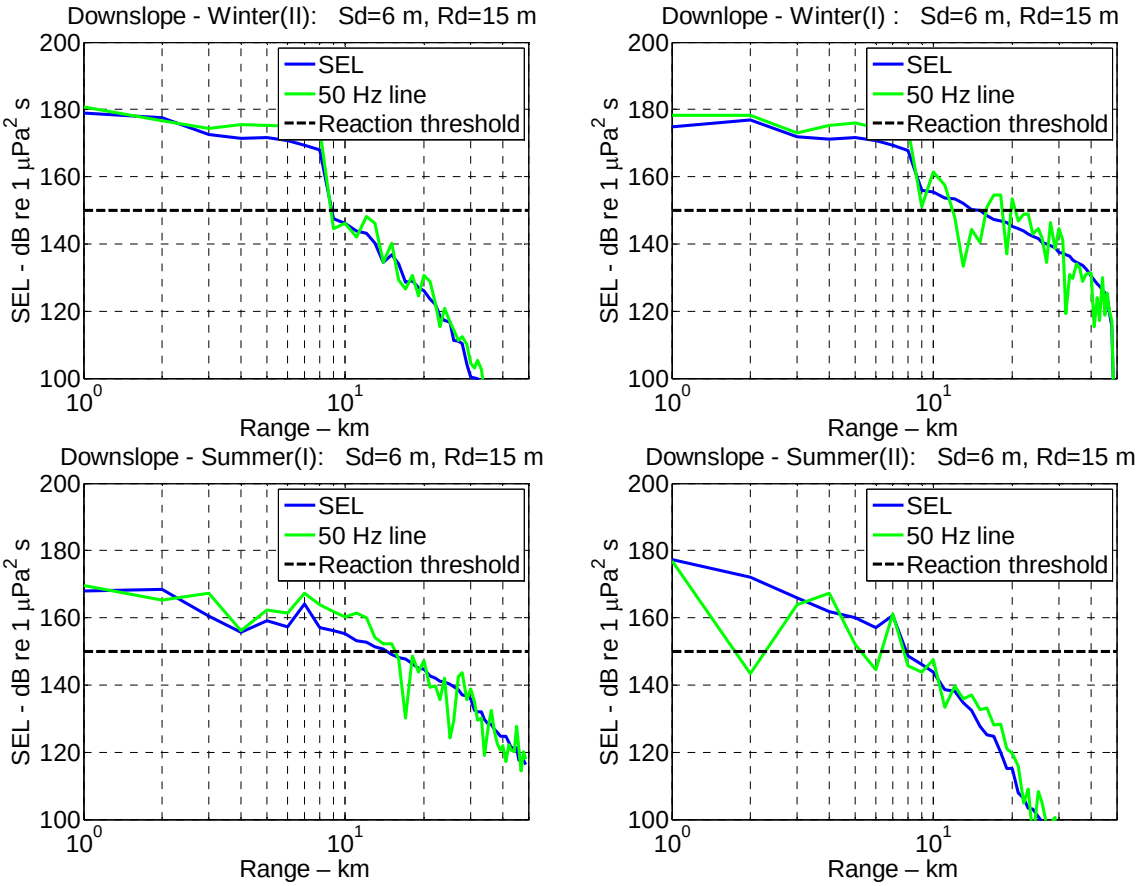

Figure 24. SEL values and spectral values for 50 Hz as function of range for downslope propagation under winter and summer conditions calculated for the bottom types (I) and (II). The dashed line is the assumed threshold value of fish reaction.

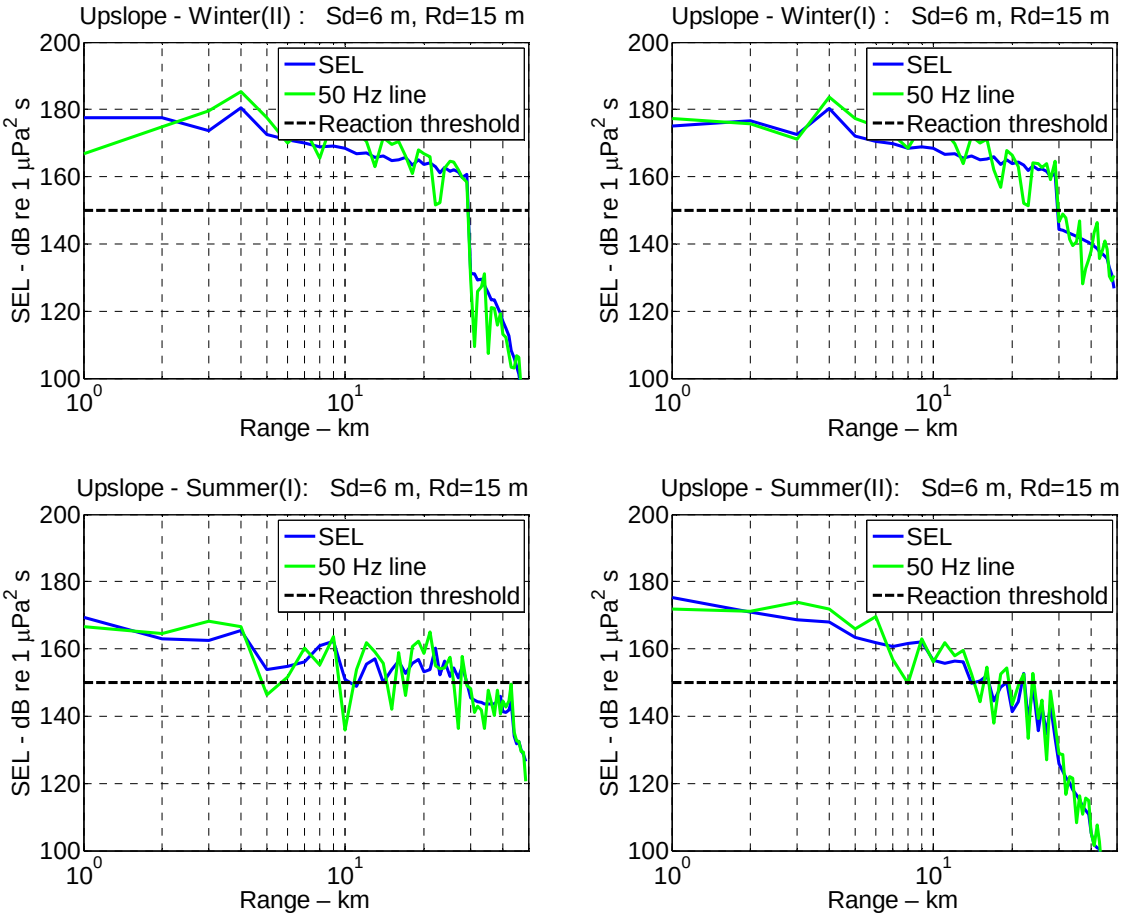

Figure 25. SEL values and spectral values for 50 Hz as function of range for upslope propagation under winter and summer conditions calculated for the bottom types (I) and (II). The dashed line is the assumed threshold value of fish reaction.

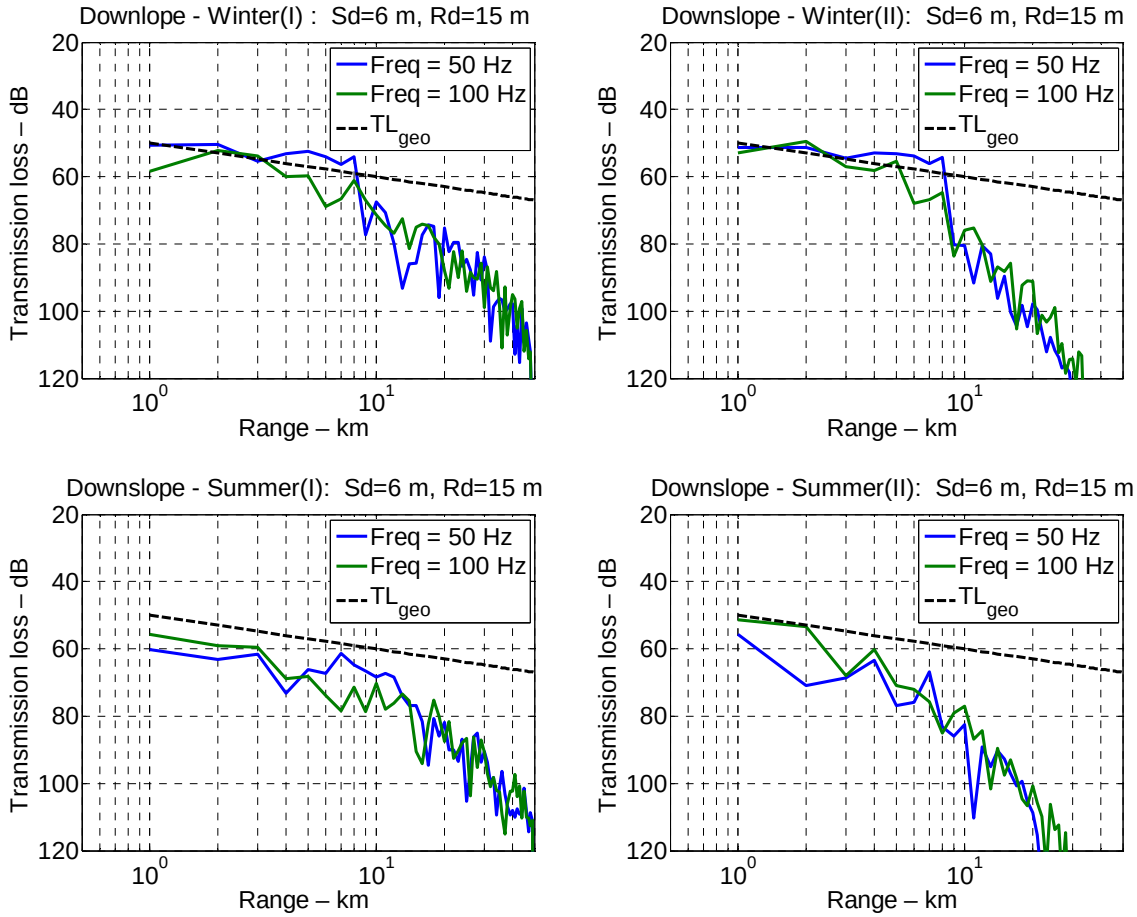

Figure 26. Transmission loss for downslope propagation under winter and summer conditions for the frequencies of 50 Hz and 100 Hz as function of range for bottom types (I) and (II).

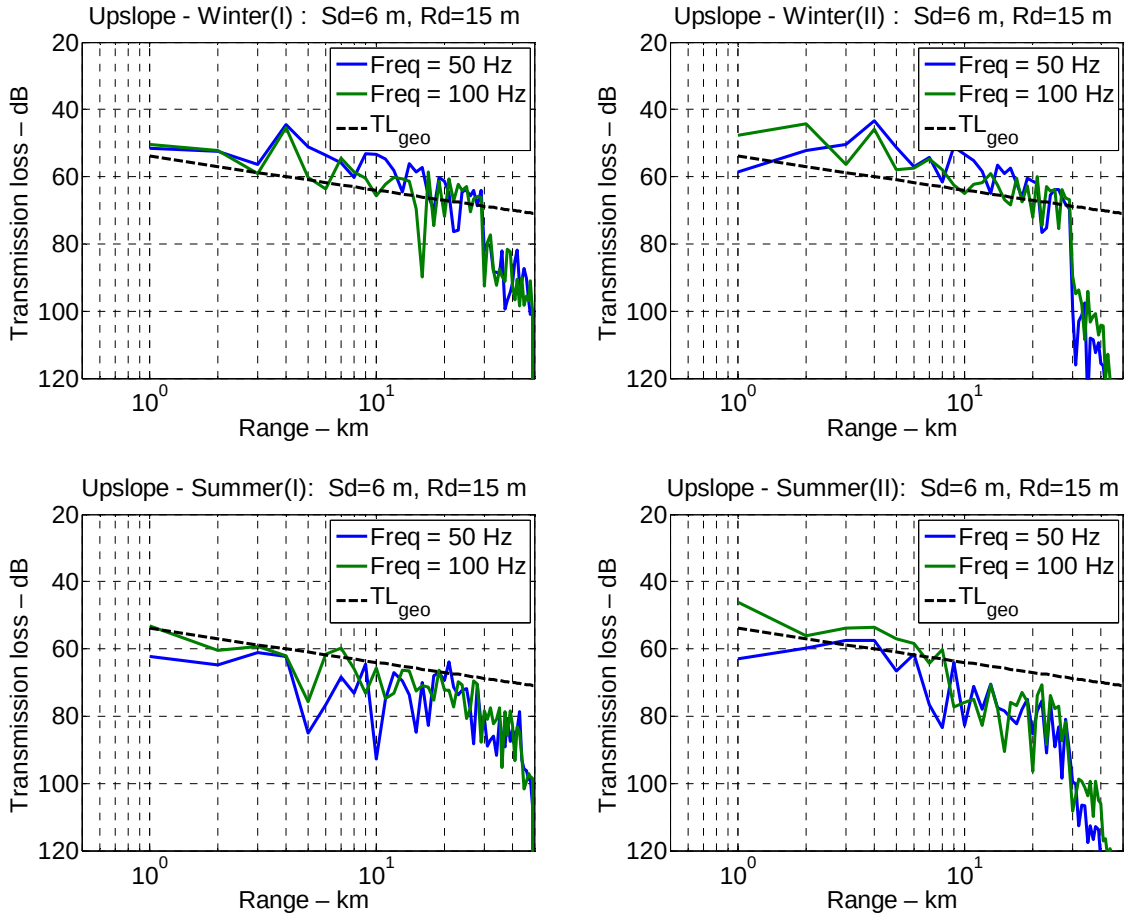

Figure 27. Transmission loss for upslope propagation under winter and summer conditions for the frequencies of 50 Hz and 100 Hz as function of range for bottom types (I) and (II).

6 Summary and conclusions

This paper describes a software model for calculating the acoustic field from airguns arrays used in marine seismic surveys for oil and gas. The model is based on ray theory and includes the effect of range dependent bathymetry and vertical variations of sound speed profiles. The bottom is represented with a model having a fluid-like sediment layer over a solid rock half-space and includes the effect of multiple reflection, absorption and attenuation caused by shear wave conversion. The model computes the full waveform field from the air gun signals allowing for comparison with recorded signals. The propagation model has been extensively tested against other models based on wavenumber integration technique and found to be accurate for frequencies above 25 Hz, which is sufficient for application to fish of interest to commercial fishing. Furthermore, the model has been validated with very good agreements by comparison with field measurements from an airgun survey over a 30 km track with significant depth variation.

The model is intended for prediction of sound field characteristics for comparison with reaction criteria of fish in order to estimate the critical distance for disturbance. Two reaction criteria for disturbance has been implemented and discussed in the paper; a criterion based on the sound exposure level and another based on the spectral levels of selected frequency components. Since the model computes the full wave form of the signals, new measures or criteria can easily be implemented as new knowledge is gained.

The propagation of underwater sound is very dependent on the environmental conditions, in particular the oceanographic parameters, the topography of the seafloor and the physical properties of the bottom. By a series of examples these effects are discussed qualitatively and quantitatively in terms calculation the critical range. The paper has studied the effects of (1) seasonal variations in the sound speed profile, (2) the geophysical properties of bottom, including absorption and shear wave conversion and (3) the bathymetry or the change of depth over propagation track.

Some of the more important conclusions are:

(1) The directionally of the airgun array is important, also at low frequencies. Using the configuration of a real array, the level in the horizontal direction is found to be 5 dB a lower than the in the vertical direction at 50 Hz, at 100 Hz the difference is about 15 dB.
(2) Sound channeling effects may be lead to exceptionally good propagation to very large distances. In northern waters the sound channels are likely to appear at very shallow depths, also at depth of the airguns.
(3) The bottom reflection loss is of outmost importance, a fact well known by acousticians, but apparently not recognized by marine biologist. Especially important is the reflection loss for low frequencies and near-horizontal incident angles where the reflection loss is determined by shear wave conversion and absorption to a depth in the bottom of at least 25 m.

(4) Water parameters are coupled with the bottom parameters in the way they affect sound propagation. For instance, the bottom reflection loss is more important in combination with a downward refracting sound speed profile than with an upward refracting profile. Hence, the impact of the bottom properties may be seasonal dependent.

(5) The critical distance is defined as the maximum distance where the sound level exceeds a predefined threshold. The critical distances calculated in the examples are based on a reaction threshold close to the startle threshold of cod, which is some 60-70 dB higher than the auditory threshold. The discussion on the "correct" threshold values for behavior reactive is on-going and controversial and the values for the critical distances given in this paper should not in any way be considered as authoritative.

References

Caldwell, J. and W. Dragoset (2000). A brief overview of seismic air-gun arrays. The leading Edge, vol. ***19****(8): p. 898-902.*

Carey, W. M., (2006) Sound sources and levels in the ocean. Oceanic Engineering, IEEE Journal of, vol ***31****(1): p. 61-75.*

Chapman ,C. J. and A. D. Hawkins, (1973) A field study of hearing in the cod, Gadus morhua. L. J. Comp. Physiol., vol. 85: p. 147-167.

Chapman, C. J., (1973) A field study of hearing in teleost fish. Helgol. Wiss. Meersunters, vol. ***24****: p. 371-390.*

Eaton, R. C J. G. Canfield, and A. L. Guzik(1995), Left-right discrimination of sound onset by the Mauthner system. Brain Behav. Evol. Vol. 46: p. 165-179.

Erbe, C, and Farmer, D.M. (2000a). *A software model to estimate zones of impact on marine mammals around anthropogenic noise.* J. Acoust. Soc. Am. Vol. 108 1327-31.

Erbe, C, and Farmer, D.M. (2000b). *Zones of impact around icebreakers affecting beluga whales in the Beaufort Sea*. J. Acoust. Soc. Am. vol. 108, 1332-40.

Francois, R. E. and G. R. Garrison (1982), *Sound absorption based on ocean measurements. Part II: Boric acid contribution and equation for total absorption*. J. Acoust. Soc. Am. vol. 72: p. 1879-1890.

Fugro - Geoteam AS (2000)., *Energy source layout for R/V "GEO PACIFIC".* PA-A2-3460-60-R-2000, project No 35374.

Hamilton E. L. and R. T. Bachman (1982), *Sound velocity and related properties of marine sediments,* J. Acoust. Soc. Am. vol. 72(6): p. 1891-1904.

Hamilton, E.L. (1987) *Acoustic Properties of Sediments*, in *Acoustics and Ocean Bottom*, L. Lara-Sáenz, Prof., C. Ranz-Guerra, Dr., and C. Carbó-Fité, Dr., Editors., Consejo Superior de Invertigaciones Cientificas (C.S.I.C.): Madrid.

Hovem Jens M. (2008)., *PlaneRay: An acoustic underwater propagation model based on ray tracing and plane wave reflection coefficients*, in Theoretical and Computational Acoustics 2007, Edited by Michael

Taroudakis and Panagiotis Papadakis, Published by the University of Crete, Greece, pp. 273-289, (ISBN: 978-960-89785-4-2).

Hovem, J.M., M.D. Richardson, and R.D. Stoll. (eds.) (1991) "Shear waves in marine sediments". Kluwer Academic Publishers 1991 ISBN 0-7923- 1357- 7.

Hovem, Jens M. Hans Erik Karlsen, Tron Vedul Tronstad and Svein Løkkeborg, (2012). *Modeling propagation airgun sounds and the effects on fish behavior*. Accepted for publication in in IEEE Journal of Ocean Engineering, May 2012

Hovem, Jens M., (2011), *Ray trace modeling of underwater sound propagation- documentation and use of the PlaneRay model*. SINTEF Report A21539, ISBN 978-82-14-04997-8, 2011-11-23

Hovem, Jens M., (2012). "Marine Acoustics−The Physics of Sound in Marine Environments" ISBN 9780932146656, Peninsula Publishing, Los Altos, CA, USA. In press, June 2012

Jensen F. B., W. A. Kuperman, M. B. Porter, and H. Schmidt, (1994).*Computational Acoustics*, AIP Press, New York Jersey,

Karlsen, H. E., W. Piddington, P. S. Enger, and O. Sand, *Infrasound initiates directional fast-start escape responses in juvenile roach Rutilus rutilus*. J. Exp. Biol., 2004. **2007**(4185-4193).

Løkkeborg, S., E. Ona, A. Vold, H. Pena, A. Salthaug, B. Totland, J. T. Øvredal, J. Dalen, and N. O. Handegard, (2010) *Effects of seismic surveys on fish distribution and catch rates of gillnets and longlines in Vesterålen in summer 2009*. Fisken og Havet No 2, The Institute of Marine Research.

NGU. *Classification of sediments based on grain size composition*. (2009) [cited 2010 June 15]; Available from: http://www.ngu.no/Mareano/Grainsize.html.

Pearson, W. H., J. R. Skalski, and C. I. Malme, (1992) *Effects of sounds from a geophysical survey device on behaviour of captive rockfish (Sebastes spp.)*. Can. J. Fish. Aquat. Sci., vol. **49**: p. 1343-1356.

Popper, A. N., R. R. Fay, C. Platt, and O. Sand, (2003) *Sound detection mechanisms and capabilities of teleost fishes*, in *Sensory Processing in Aquatic Environments*, S. P. Collin and N. J. Marshall, Editors. Springer-Verlag, New York, 2003, p. 1-38.

Schmidt, H., (1987) *SAFARI: Seismo-acoustic fast field algorithm for range independent environments*. User's guide, SR-113, SACLANT Undersea Research Centre, La Spezia, Italy.

Simmonds, J and D. MacLennan.(2004). "Fishery Acoustics. Theory and Practice", Blackwell Publishing, Oxford, UK.

Tronstad Tron Vedul and Jens M. Hovem (2011), *Bathymetric and seasonal effects on propagation of airgun signals to long distances in the ocean.* OCEANS'11 MTS/IEEE, Kona, Hawaii, Sept. 19 – 22.